JOURNAL OF GEOPHYSICAL RESEARCH, VOL. 104, NO. A5, PAGES 10,111–10,118, MAY 1, 1999

Schumann resonance parameter changes during high-energy particle precipitation

K. Schlegel
Max-Planck-Institut für Aeronomie, Katlenburg-Lindau, Germany

M. Füllekrug
Institut für Meteorologie und Geophysik, Universität Frankfurt, Frankfurt, Germany

Abstract. A systematic study of Schumann resonance parameters during high-energy particle precipitation events is presented. Protons and electrons with energies above 1 MeV ionize the upper boundary of the Earth-ionosphere cavity, leading to an increase of the resonance frequency and a decrease of the damping of the first Schumann resonance, as derived from measurements at Arrival Heights, Antarctica. The study uses the nine strongest solar proton events of the past solar cycle 22 and high-energy electrons emitted periodically from corotating interaction regions in the solar wind during 1994–1995. The variation of the Schumann resonance parameters is in qualitative agreement with current theories of Schumann resonances. The study also shows that high-energy particle precipitation is not the only relevant source affecting Schumann resonance parameters. The reported findings constitute a so far little-explored aspect of solar terrestrial relations.

1. Introduction

Schumann resonances (SR) are resonant electromagnetic waves in the Earth-ionosphere cavity with a fundamental frequency of about 8 Hz and higher-order modes separated by ~6 Hz. After their prediction and theoretical discussion by *Schumann* [1952] they have been extensively studied during the past decades (e.g., *Sentman* [1995], for a recent review). It is commonly assumed that cloud-to-ground lightning discharges from global thunderstorm activity are the main excitation sources of SR.

The Earth-ionosphere waveguide is defined by the conducting boundaries of the Earth's surface ($\sigma \approx 10^{-3}$ S m^{-1}) and the lower part of the ionosphere ($\sigma \approx 10^{-4}$–10^{-2} S m^{-1}) at ~80 km height, whereas the conductivity in between is very low with values $\sigma < 10^{-10}$ S m^{-1} (see Figure 4 below). Changes of the D region ionization lead to conductivity changes and may thereby modify parameters of the SR.

The regular diurnal variation of the D region ionization results from solar zenith angle variations. Superimposed strong ionization changes may occur, for example, during high-energy particle precipitation. They can enhance the D region electron density down to 60–50 km altitude, depending on the particle energy [e.g., *Collis and Rietveld*, 1990; *Schlegel*, 1995]. Although these effects are long known and well understood, only a few papers have addressed the consequences for SR. *Ogawa and Tanaka* [1970] reported an anticorrelation between SR Q factors of the first two modes and sunspot numbers from observations between February 1976 and January 1968. *Sentman* [1991] and *Sentman et al*. [1996] examined SR measurements from California and Australia during large solar storms in the fall of 1989. They found no measurable response in the SR intensities but also found a sudden decrease in Q factors of the second mode, which they attributed to small changes of the middle atmospheric conductivities by energetic particles. The present study continues and extends these early attempts to establish a correlation of solar activity and SR parameters, covering almost a whole solar cycle.

Copyright 1999 by the American Geophysical Union.

Paper number 1999JA900056.
0148-0227/99/1999JA900056$09.00

2. Schumann Resonance Data

The SR are measured as part of the Stanford ELF/VLF Radio Noise Survey, which provides a variety of information on the anthropogenic and natural electromagnetic environment [*Fraser-Smith et al*., 1991]. This study uses measurements of one horizontal magnetic component oriented in the geographic north-south direction at Arrival Heights, Antarctica (78°S, 167°E). The data analysis is based on half hourly sampled time series of 52 s lengths. The SR parameters resonance frequency, damping, and amplitude are derived by use of a robust version of the complex exponential algorithm [*Füllekrug*, 1995] which relies on Prony's method [*Marple*, 1987]. This algorithm determines the SR parameters in three steps. (1) The autoregressive coefficients of the process are determined from the autocovariance function. (2) A z transform of the autoregressive coefficients yields the internal parameters of the resonance system, that is, the damping and frequency of the Earth-ionosphere cavity. (3) The parameters of the excitation source, that is, the amplitude and phase, are finally determined by fitting a damped oscillation with the specified frequency to the autocovariance function. In this way, the complex exponential algorithm determines all free parameters of the SR, and the frequency, in particular, while the conventional Fourier transform is restricted to a frequency resolution $1/T$, determined by the length of the analyzed time interval T. The derived parameters of the SR may be used to describe their spectrum in the frequency domain where the frequency and damping are represented by the center and width of the spectrum, respectively. The accuracy of this complex exponential algorithm is mainly determined by the stationarity of the

spectrum. Tests of the algorithm with varying time intervals T between 1 and 15 min indicated maximum variations of the SR parameters $< 5\%$. It follows from the algorithm that the frequency and the damping of the SR are given in hertz and the amplitude is given in picoteslas. While the amplitude and phase describe the excitation of SR, the damping and the observed frequency are determined by ionospheric boundary conditions and the source-observer geometry. These parameters are summarized in daily mean values for this study.

3. High-Energy Particles

The term "high-energy" particles is used in different ways. Auroral keV particles, accelerated in the magnetosphere and precipitating during geomagnetic storms down to the thermal ionospheric plasma, are usually denoted high-energy particles. The subjects of this study, however, are particles with three to five orders of magnitude larger energies which are accelerated in the solar corona.

Protons with energies up to 100 MeV are most often emitted from the Sun in conjunction with solar flares [*Ellison and Ramaty*, 1985]. Proton emissions may persist for many days, while the duration of optical and X-ray flares is usually <1 hour. These solar proton events (SPE) cause additional ionization in the D region over large circular-shaped areas centered on the geomagnetic poles because of the influence of the geomagnetic field on the particles. This additional ionization causes radio blackouts [*Satori*, 1991] over these areas and was therefore called a polar cap absorption (PCA) event [*Bailey*, 1964].

Together with strongly enhanced fluxes of high-energy protons, electrons with energies >1 MeV are usually emitted after flares. These high-energy electrons can also penetrate deep into the D region and cause additional ionization. They are often called solar electron events (SEE) or solar relativistic energy events in the scientific literature. Ionospheric effects caused by SPE and SEE can usually not be separated during the days following a flare.

Another class of high-energy electrons are accelerated in the corotating interaction regions (CIRs) of the solar wind [*Andersen et al.*, 1995; *Sarris and Krimigis*, 1985]. These CIRs may be active at considerable distances from the Sun (several AU), so that the accelerated particles reach the Earth from the "back" (with respect to the Sun). CIRs are particularly well developed during the years of minimal solar activity and produce reoccurring bursts of high-energy electrons with a period of 26–28 days caused by the solar rotation. These bursts were particularly well defined in the first half of 1994; the corresponding data are used in this study (section 5, Figure 3). In this case the ionospheric effects of the high-energy electrons can be clearly identified, because only one short-lived SPE was observed during this time period (February 1994; last line in Table 1, horizontal bar in Figure 3). In the following text we keep the term SEE for convenience to describe these high-energy electrons, although the electrons are not accelerated directly on the Sun.

Proton and electron fluxes with $E > 1$ MeV are routinely measured with the space environment monitor system on board the GOES satellites. The data are available from the SPIDR database through the Internet (http://spidr.ngdc.noaa.gov:8080/production/html/GOES/index.html).

4. SPE-Related Changes to SR Parameters

Figure 1 shows two examples of the observed changes in SR parameters associated with SPE. The first row displays daily mean values of the proton flux F_p. The events represent the strongest SPEs (in terms of peak particle flux) of the past solar cycle 22. The peak flux on October 20, 1989, was 53,720 counts $cm^{-2}\ s^{-1}\ sr^{-1}$; on March 25, 1991, it was 29,860 counts $cm^{-2}\ s^{-1}\ sr^{-1}$. The sudden increase of the SR frequency is evident in the second row of plots. In both cases it amounts to about 0.12 Hz. The damping (third row of plots) indicates a slight decrease in both cases. Finally, the amplitude changes displayed in the fourth row are very distinct for the 1989 event but less clear for the 1991 event.

Table 1 summarizes the results of an analysis of the 9 strongest SPE of solar cycle 22 (for another strong event in August 1989, no SR data were available). The duration of the events (column 2) was defined as the time interval during which the proton flux exceeded 300 counts $cm^{-2}\ s^{-1}\ sr^{-1}$. The results of our analysis indicated that fluxes below this limit did not cause any SR parameter changes. To estimate the changes of SR parameters for each individual event, the background was calculated as an average from at least 10 days before and after the indicated duration interval in Table 1. The parameter change was then calculated as the difference between the peak values during the event and this background. Long-term averages of the SR frequency, damping, and amplitude are 7.5 Hz, 0.5 Hz, and 1.0 pT, respectively. Again, it is obvious from the values of Table 1 that the peak flux on one hand and the changes of the SR parameters on the other hand are not perfectly correlated.

Even though the strongest SPEs have been used, the changes in the SR parameters are small compared to their diurnal variation [*Füllekrug*, 1995]. Day-to-day variations of the D region electron density, for example, through mesospheric winds and planetary waves, and the SR frequency dependence on the distance to the lightning activity [*Madden and Thompson*, 1965] result in statistical fluctuations and may mask significant SR parameter variations.

In order to make the particle-induced changes of the SR parameters more clearly visible we have performed a superposed epoch analysis of the nine SPEs listed in Table 1. For this purpose we used the day with the maximal proton flux as "key day." Figure 2 (left plots) clearly shows the mean decrease of the damping and the increase of the frequency and the amplitude compared to the SPE flux F_p.

5. SEE-Related Changes to SR Parameters

Figure 3 shows the influence of SEEs on SR parameters. In the first plot, daily means of electron flux ($E > 1$ MeV) are plotted for the first 250 days of the year 1994. The periodicity of 26–28 days resulting from the solar rotation is very pronounced in the first 180 days of this year; later, shorter periods dominate. The same periodicity can be ascertained in the frequency (second plot). It is superimposed on a systematic annual variation which has already been studied (for SR intensity: *Märcz et al.* [1997]; for SR amplitudes: *Satori and Zieger* [1996]). The solar rotation period is less pronounced in the third and fourth plots showing daily means of the SR damping and amplitude.

In order to enhance the signal-to-noise ratio of the analysis we applied the superposed epoch analysis to 24 events during the years 1994–1995, using the day with the strongest electron flux increase as key day. Figure 2 (right plots) shows the mean

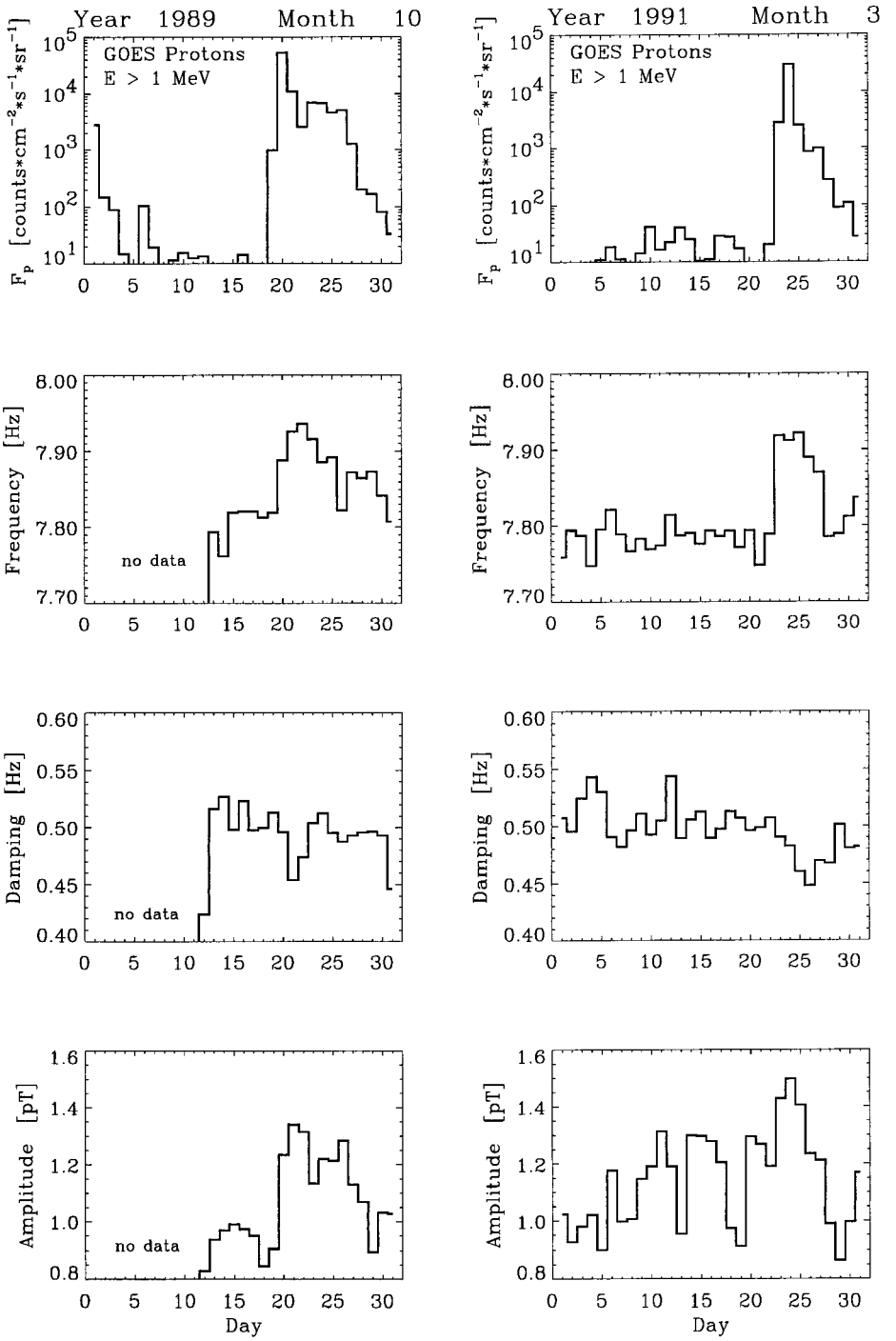

Figure 1. Comparison of proton flux (first row), SR frequency (second row), SR damping (third row), and SR amplitude (fourth row) for two strong solar proton events (SPEs) in October 1989 and March 1991. Plotted are daily means of the four quantities versus day of the month.

decrease of the damping and the increase of the frequency and amplitude compared to the electron flux F_e. The observed SR parameter changes clearly exhibit the 26–28 day solar rotation period. The deviation from the background for frequency and damping is approximately half as large as the deviation for the mean SPE event in the left plots of Figure 2; the amplitude deviation is even smaller. Note that the ordinates in Figure 2 cover the same range intervals for the SPE and the SEE in order to facilitate the comparison.

6. Discussion in Terms of Current Theories

According to a widely accepted theory proposed by *Sentman* [1990], the SR frequencies can be expressed as

$$f = \sqrt{\frac{n(n+1)}{2\pi}}\,\frac{c}{r_e}\,\sqrt{\frac{h_1}{h_2}} \tag{1}$$

Here n is the mode number (only $n = 1$, the first harmonic, is regarded here), c is the velocity of light, r_e is a mean Earth

Table 1. The Nine Strongest Solar Proton Events During Solar Cycle 22 and Corresponding Schumann Resonance Parameter Changes

Solar Proton Event	Duration, days of month	Peak Flux, 10^3 counts $cm^{-2}\ s^{-1}\ sr^{-1}$	Frequency Increase, Hz	Damping Decrease, Hz	Amplitude Increase, pT
March 1989	9–13	7.9	0.07	0.04	0.41
October 1989	19–27	53.72	0.12	0.04	0.39
Nov.–Dec. 1989	27–3	11.10	0.12	0.02	0.37
March 1991	23–28	29.86	0.14	0.05	0.34
June 1991	1–18	6.47	0.05	0.05	−0.06
July 1991	8–11	20.73	0.04	0.02	0.17
Oct.–Nov. 1991	18–5	15.58	0.05	0.05	0.11
May 1992	9–11	9.62	0.07	0.03	0.14
Feb. 1994	20–22	13.73	0.09	0.04	0.23

radius, and h_1 and h_2 are two characteristic heights in the D region. At $h_1 \approx 40$–50 km the conduction and displacement currents are of the same order of magnitude and the atmospheric conductivity is $\sigma = \varepsilon_0\omega$. At $h_2 \approx 75$–90 km the high atmospheric conductivity determines the reflection boundary where the local conductivity scale height s_2 approximately equals the inverse wave number of the mode; that is,

$$\sigma_2 = 1/(4\mu_0\omega s_2^2) \tag{2}$$

If we assume that the high-energy particle precipitation decreases the height h_2 by an amount δ because of the additional ionization,

$$f = \text{ const } \sqrt{h_1/(h_2 - \delta)} \tag{3}$$

and that h_1 remains approximately constant, then for the relative frequency increase it follows that

$$\Delta f/f \approx \delta/(2h_2) \tag{4}$$

The amount of δ depends on the flux of the high-energy particles causing the additional ionization. Using $\Delta f = 0.12$ Hz (from the October 1989 SPE), $f = 7.5$ Hz, and $h_2 = 80$ km yields $\delta_g = 2.5$ km. The subscript g stands for global here, since the frequency increase is assumed to be a global effect.

Figure 4 shows conductivity profiles for various conditions. Below 60 km the conductivity was taken from a model by *Volland* [1984] because actual measurements are rare. The undisturbed D region conductivity (dotted line) was estimated with the relation

$$\sigma = \varepsilon_0(\omega_i^2/\nu_i + \omega_e^2/\nu_e) \tag{5}$$

using an electron density profile from the international reference ionosphere (IRI) for afternoon equinox conditions to calculate the ion and electron plasma frequencies ω_i and ω_e (assuming $n_i = n_e$). The collision frequencies ν_i and ν_e have been taken from *Volland* [1984, Figure 2.3]. During the main phase of the October 1989 SPE the EISCAT incoherent scatter facility in Tromsö, Norway, measured electron density profiles between about 50 and 90 km altitude [*Collis and Rietveld*, 1990, Figure 6]. Using this profile and (5) yields the conductivity profile indicated by a solid line in Figure 4. Comparing this profile with the undisturbed one reveals that the conductivity level usually present at $h_2 = 80$ km is downshifted by about 12 km during the particle precipitation.

This value of δ seems to be a contradiction to the value of 2.5 km estimated above from the frequency increase. Both numbers can be reconciled however, regarding the following:

1. *Sentmen*'s [1990] formula (equation (1)) applies only to globally averaged heights. The value of $\delta_g = 2.5$ km derived via this formula therefore has to be regarded as a global height shift.

2. The particle precipitation occurs only over extended polar caps (compare section 3), and the European Incoherent Scatter (EISCAT) observations ($\phi = 69.4°$N, $\lambda = 19.1°$E) are within the area affected by the PCA precipitation. The value $\delta_{PC} = 12$ km, derived from the density profile, applies therefore only to the polar cap.

If one further assumes that during the strong PCA event of October 1989 the polar cap extended down to about 55° latitude (this value is comparable with the extent of strong PCA effects obtained from measurements with riometer chains [*Ranta et al.*, 1993]), then the area of two of such extended polar caps amounts to about 20% of the total global D region. This number matches approximately the ratio of 2.5/12 of the two height shifts. This is, of course, a very crude approximation, but it points to the right direction. It should also be noted that during very strong SPE the height h_1 may be downshifted by a small amount as well. In this case our value of δ_g would be underestimated.

A more quantitative explanation of the frequency shift needs a detailed global model with a nonuniform upper (ionospheric) boundary of the waveguide, which is not yet available. *Galeis* [1972] treated the case of day-night asymmetries but not the PCA case. The latter was studied by *Bliokh et al.* [1980]. According to their theory, the PCA event would cause a splitting of the SR modes, resulting in a somewhat reduced frequency. This is contradictory to our results.

Figure 4 also displays a conductivity profile calculated for a strong SEE (dash-dotted line), again from EISCAT electron density data, obtained on April 13, 1994 (this day is marked in Figure 3 with a little arrow). The conductivity in the 65–80 km height range is quite similar to the one in the SPE case, which may explain the similar frequency increases during SPE and SEE. It should also be remembered that after solar flares, high-energy protons are almost in every case associated with high-energy electrons, while the SEE regarded here are not necessarily accompanied by high-energy protons. The conductivity profiles obtained during SPEs therefore contain, in most cases, ionization effects of SEE too.

The damping of the SR shows a clear decrease. This decrease may qualitatively be explained with reduced losses within the Earth-ionosphere cavity. A quantitative check is hardly possible because the damping depends on two unknown

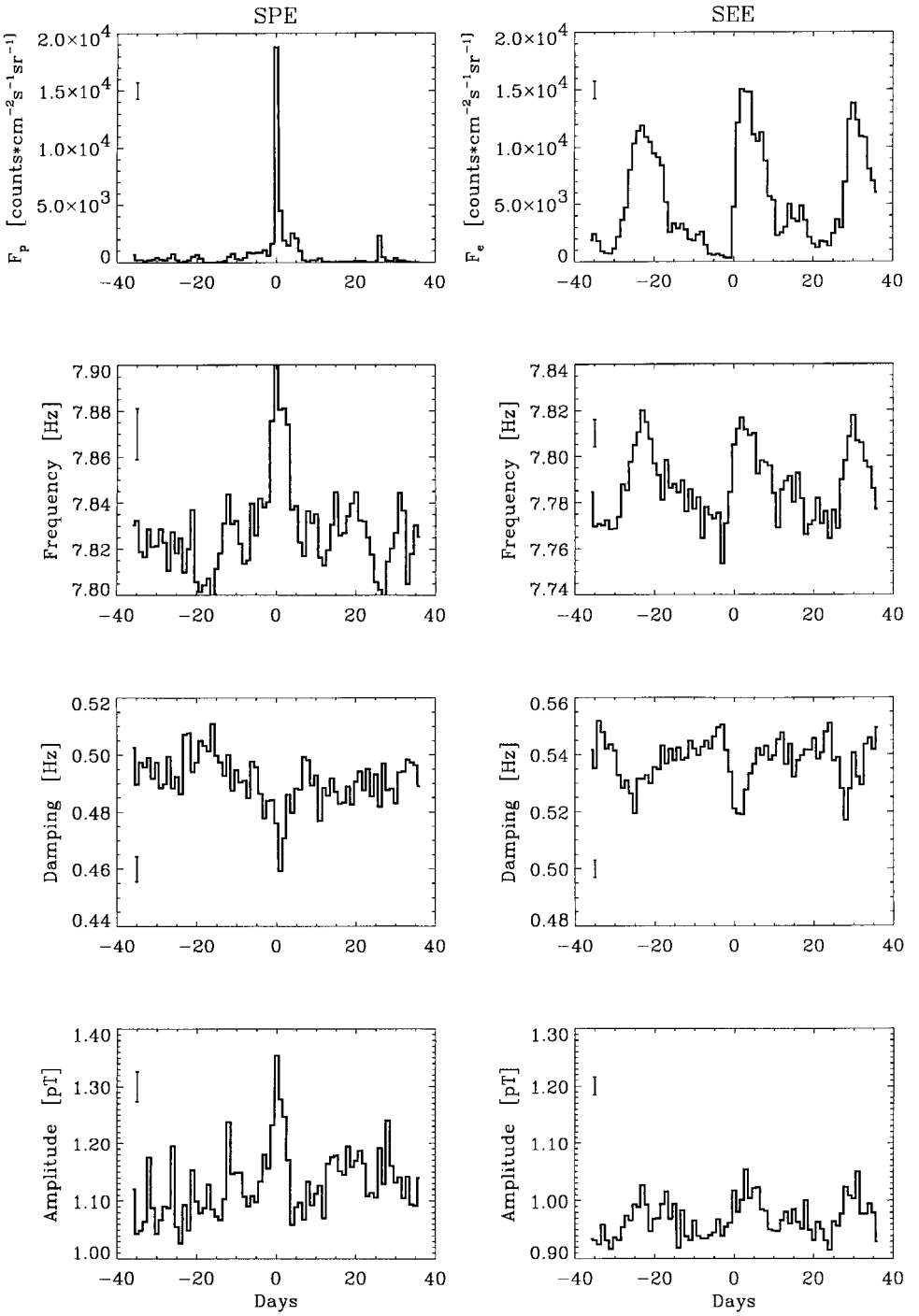

Figure 2. Superposed epoch analysis of nine SPEs during solar cycle 22 (left plots) and 24 SEEs during 1994–1995 (right plots). The first plot shows the proton (F_p) and electron (F_e) flux, and the succeeding plots show the Schumann resonance parameters frequency, damping, and amplitude. The deviations from the background are approximately twice as large for SPEs compared to SEEs. The error bars in the corner of each plot indicate an average standard deviation from the plotted mean values.

parameters s_1 and s_2. According to *Sentman* [1990], the damping can be expressed as

$$D = \text{const}(s_1/h_1 + s_2/h_2) \tag{6}$$

If we use our results that D is slightly decreased during disturbed conditions, we can only infer that the two scale heights s_1 (around h_1) and s_2 (around h_2) must become flatter when h_1 (quiet) $\approx h_1$ (disturbed) and h_2 (quiet) $\approx h_2 - \delta$ (disturbed), in agreement with the profiles of Figure 4.

The large observed amplitude increase during the SPE can only be explained qualitatively. According to current understanding, the diurnal variation of the SR amplitude is mainly determined by the variability of global lightning activity. In addition, *Sentman and Fraser* [1991] attribute part of the mean

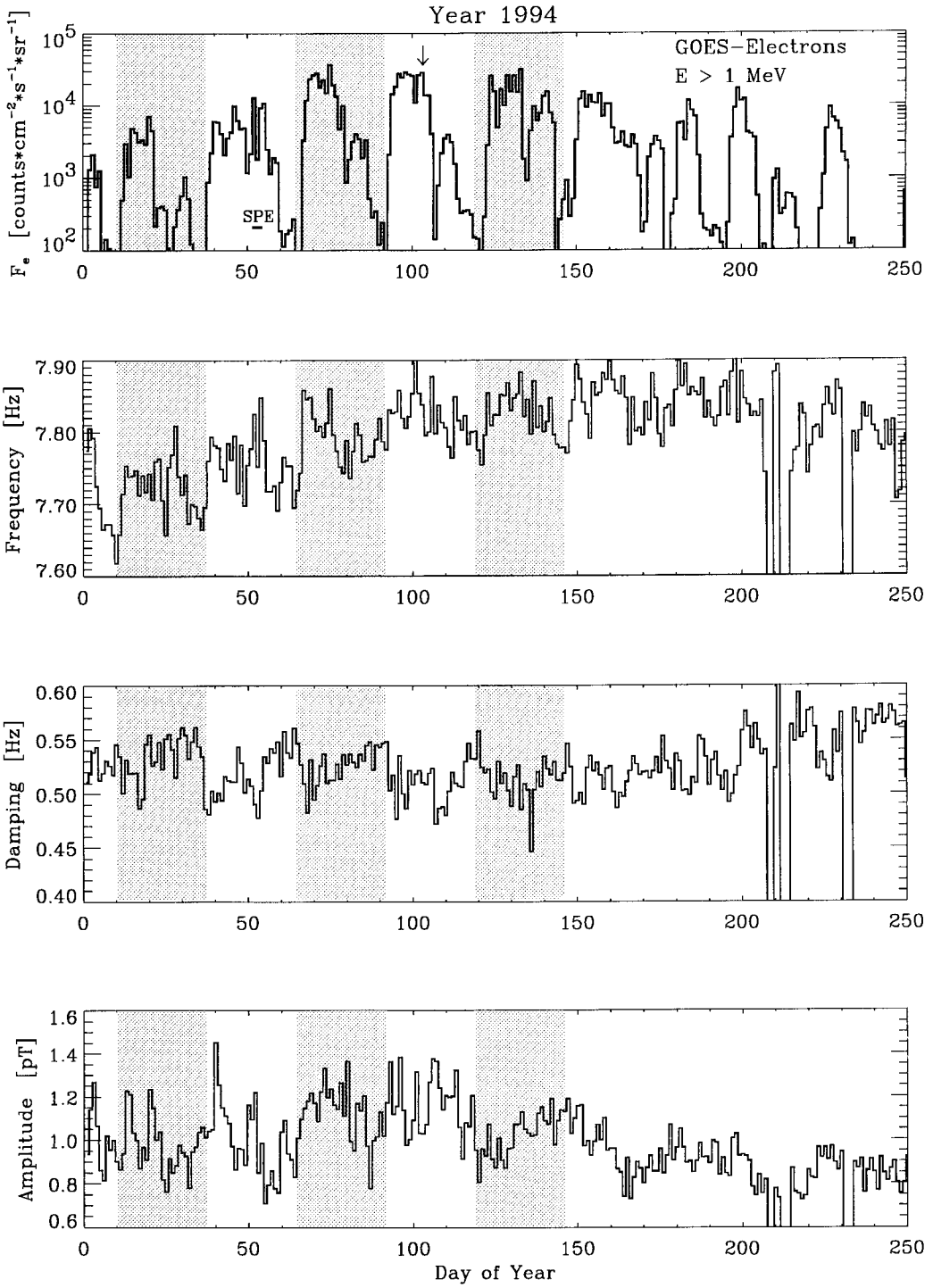

Figure 3. Similar to Figure 1 but for 180 days with periodic SEE. The arrow indicates the day for which the conductivity was plotted in Figure 4. The horizontal bar shows the duration of a SPE during this time period. The shading indicates a 27 day solar rotation period with which the electron flux is modulated.

magnetic field intensity changes to height changes of the D region. They use the relationship

$$|B|^2 = \text{const}/\sqrt{h_1 h_2} \tag{7}$$

This expression predicts an amplitude increase during particle precipitation, when $h_2 \rightarrow h_2 - \delta$. If we insert the above used numbers (h_2 = 80 km, δ = 2.5 km), however, the inferred amplitude change should only be about 1%; actually, it is up to 40% (see Table 1). Even an additional decrease of h_1 by a few kilometers would not explain the large observed amplitude changes.

The increase of SR amplitudes observed during high-energy particle precipitation events is relatively small compared to the diurnal variation which results from global lightning activity

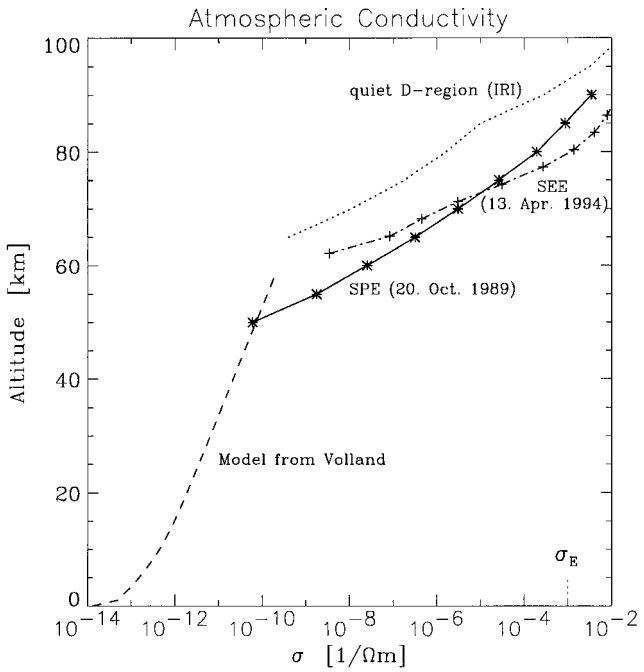

Figure 4. Conductivity profiles for different conditions. The dashed curve represents a model described by *Volland* [1984]. The dotted line characterizes the quiet-time *D* region conductivity estimated from international reference ionosphere (IRI) model electron densities. The solid line shows the conductivity profile obtained from European Incoherent Scatter (EISCAT) data during a strong SPE; the dash-dotted line is from EISCAT data for a strong SEE. The average conductivity of the Earth surface is indicated in the lower right.

changes. It is commonly assumed that the ionosphere acts as a filter which divides the naturally occurring waves in magnetospheric micropulsations at frequencies < 4 Hz and ELF sferics of atmospheric origin at frequencies > 4 Hz. On the other hand, globally correlated amplitude variations of the SRs associated with the solar rotation period have been reported and attributed to geomagnetic activity [*Füllekrug and Fraser-Smith*, 1996]. In this view, the considered frequency range represents a transitional band where both excitation sources contribute to the wave phenomena observed at the surface of the Earth. Therefore the amplitude changes reported in this contribution may be also related to the local enhancement of high-frequency micropulsations associated with auroral keV electron precipitation. This will be subject to further studies.

7. Summary and Conclusions

The presented results show that SR parameters are indeed affected by energetic solar particles. In the case of solar proton events (SPE) (1) the SR frequency increases by about 0.04–0.14 Hz, depending on the intensity of the proton flux, with respect to a mean value of ~7.8 Hz, (2) the SR damping decreases by about 4–10% from a mean value of ~0.5 Hz, and (3) the SR amplitude increases by several 10% from a mean value of ~1.1 pT. Whereas the frequency increase and the damping decrease can by qualitatively explained by current theories, we cannot provide a satisfactory explanation for the amplitude increase.

In the case of solar electron events (SEE) the character of the SR parameter variations is the same, but their magnitude is considerably smaller. This can be explained by the fact that the electrons affect the conductivity profile less than the protons do (see Figure 4).

The effects reported here represent a channel of solar terrestrial relationships which was not sufficiently studied before. Since SR parameter variations can be measured at any place on Earth, provided the man-made interference is sufficiently low, the consequences of high-energy particle precipitation events may be globally observable. In contrast, the *D* region ionization enhancements of SPE and SEE are relatively localized, depending on latitude and, in the case of the electrons, also on local time. Although we do not see any major impact of this channel of solar influence on Earth, its study is nevertheless important in order to complete our understanding of the various aspects of solar terrestrial relations.

Acknowledgments. We are grateful to Fraser-Smith for providing the SR data from ARRIVAL HEIGHTS. We thank the EISCAT Director and staff for running the radar and providing the data. EISCAT is a Scientific Organization funded by national scientific agencies of Finland, France, Germany, Japan, Norway, Sweden, and the United Kingdom. We also thank Dan Wilkinson for his help in providing the GOES data.

Michel Blanc thanks both referees for their assistance in evaluating this paper.

References

Anderson, K. A., J. Sommers, R. P. Lin, M. Pick, P. Chaizy, N. Murphy, E. J. Smith, and J. L. Philips, Mirroring of fast solar flare electrons on a downstream corotating interaction region, *J. Geophys. Res.*, *100*, 3–11, 1995.

Bailey, D. K., Polar-cap absorption, *Planet. Space Sci.*, *12*, 495–541, 1964.

Bliokh, P. V., A. P. Nickolaenko, and Y. F. Fillipov, *Schumann Resonances in the Earth-Ionosphere Cavity*, Inst. of Electr. Eng., London, 1980.

Collis, P. N., and M. T. Rietveld, Mesospheric observations with the EISCAT UHF radar during polar cap absorption events, 1, Electron densities and negative ions, *Ann. Geophys.*, *8*, 809–824, 1990.

Ellison, D. C., and R. Ramaty, Shock acceleration of electrons and ions in solar flares, *Astrophys. J.*, *298*, 400–408, 1985.

Fraser-Smith, A. C., P. R. McGill, A. Bernardi, R. A. Helliwell, and M. E. Ladd, Global measurements of the low frequency radio noise, in *Environmental and Space Electromagnetics*, edited by H. Kikuchi, pp. 191–200, Springer-Verlag, New York, 1991.

Füllekrug, M., Schumann resonances in magnetic field components, *J. Atmos. Terr. Phys.*, *57*, 479–484, 1995.

Füllekrug, M., and A. C. Fraser-Smith, Further evidence for a global correlation of the Earth-ionosphere cavity resonances, *Geophys. Res. Lett.*, *23*, 2773–2776, 1996.

Galeis, J., *Terrestrial Propagation of Long Electromagnetic Waves*, Pergamon Press, Tarrytown, N. Y., 1972.

Madden, T., and W. Thompson, Low-frequency electromagnetic oscillations of the Earth-ionosphere cavity, *Rev. Geophys.*, *3*, 211–254, 1965.

Märcz, F., G. Satori, and B. Zieger, Variations in Schumann resonances and their relation to atmospheric electric parameters at Nagycenk station, *Ann. Geophys*. *15*, 1604–1614, 1997.

Marple, S. L., *Digital Spectral Analysis With Applications*, Prentice-Hall, Englewood Cliffs, N. J., 1987.

Ogawa, T., and Y. Tanaka, Q factors of the Schumann resonances and solar activity, *Spec. Contrib. Geophys. Inst. Kyoto Univ.*, *10*, 21–28, 1970.

Ranta, H., A. Ranta, S. M. Yousef, J. Burns, and P. Stauning, D-region observations of polar cap absorption events during the EISCAT operation in 1981–1989, *J. Atmos. Terr. Phys.*, *55*, 751–766, 1993.

Sarris, E. T., and S. M. Krimigis, Quasi-perpendicular shock acceleration of ions to ~200 MeV and electrons to ~2 MeV observed by Voyager 2, *Astrophys. J.*, *298*, 676–683, 1985.

Satori, G., Combined ionospheric effect due to Forbush decreases and magnetospheric high-energy particles at mid-latitudes, *J. Atmos. Terr. Phys*., *53*, 325–332, 1991.

Satori, G., and B. Zieger, Spectral characteristics of Schumann resonances observed in central Europe, *J. Geophys. Res*., *101*, 29,663–29,669, 1996.

Schlegel, K., EISCAT and the EISCAT data base—A tool for ionospheric modeling (E- and D-region), *Adv. Space Res*. *16*(1), 147–154, 1995.

Schumann, W. O., Über die strahlungslosen Eigenschwingungen einer leitenden Kugel, die von einer Luftschicht und einer Ionospärenhülle umgeben ist, *Z. Naturforsch. A*, *7*, 149–152, 1952.

Sentman, D. D., Approximate Schumann resonance parameters for a two-scale-height ionosphere, *J. Atmos. Terr. Phys*. *52*, 35–43, 1990.

Sentman, D. D., Effects of the solar flares of August–October 1989 on the Schumann resonances: Evidence for large-scale, flare-induced enhancement of the lower D-region conductivity, paper presented at Joint IAGA/IAMAP Symposium on Electrodynamics of the Middle Atmosphere, Int. Council of Sci. Unions, Vienna, Aug. 1991.

Sentman, D. D., Schumann resonances, in *Handbook of Atmospheric Electrodynamics*, edited by H. Volland, pp. 267–295, CRC Press, Boca Raton, Fla., 1995.

Sentman, D. D., and B. J. Fraser, Simultaneous observations of Schumann resonances in California and Australia: Evidence for intensity modulation by the local height of the D region, *J. Geophys. Res*. *96*, 15,973–15,984, 1991.

Sentman, D. D., M. J. Heavner, D. N. Baker, T. E. Cayton, and B. J. Fraser, Effects of solar storms on the Schumann resonances in late 1989, paper presented at 10th Annual Conference on Atmospheric Electricity, Soc. of Atmos. Electr. of Jpn., Osaka, Japan, 1996.

Volland, H., *Atmospheric Electrodynamics*, Springer-Verlag, New York, 1984.

M. Füllekrug, Institut für Meteorologie und Geophysik, Universität Frankfurt, Feldbergstrasse 47, D-60323 Frankfurt, Germany.

K. Schlegel, Max-Planck-Institut für Aeronomie, Max-Planck-Strasse 2, D-37191 Katlenburg-Lindau, Germany. (schlegel@linmpi.MPG.de)

(Received June 18, 1998; revised October 24, 1998; accepted January 18, 1999.)